*International Journal on Recent and Innovation Trends in Computing and Communication*
***ISSN: 2321-8169 Volume: 11 Issue: 9s***
***Article Received:** 30 April 2023 **Revised:** 20 June 2023 **Accepted:** 20 July 2023*

# Design and Simulation of Resilient RF Receivers for 5G Interference Mitigation Using MATLAB

**Shatha Kareem Abbas, Prof. Dr. Osman Nuri Uçan**

Electrical and computer engineering department , Altınbaş University, Türkiye

corresponding author : Shatha Kareem Abbas

noorqassim100@gmail.com

**Abstract**

**Introduction:** Advanced terminal capabilities increase mobile broadband traffic, straining spectrum resources. Traditional methods like base stations are expensive. Heterogeneous networks (HetNets) using pico cells attempt to improve efficiency, however interference persists. A suggested mitigation technique uses the modified greatest weighting delay first (MLWDF) algorithm for resource allocation and reception processing, which performs well in simulations. Space, time, frequency, time-frequency, and coding domain interference reduction methods are investigated, each having hardware requirements and restrictions.
**Aim and objectives:** The study uses MATLAB to construct and simulate robust RF receivers. Enhancing 5G communication network interference reduction is the goal.
**Method:** Simulink is used to study transmitter and receiver RF losses, including I/Q imbalances, phase noise, and power amplifier non-linearity. Spectrum masks, error vector magnitudes, and peaks-to-average power ratios measure performance. Simulink models examine constellation distortion, neighboring channel rejection, and packet error rates in 802.11ax and 5G waveform reception due to RF impairments. The paper stresses the necessity of reliable data measurement for RF interference analysis and discusses interference mitigation.
**Results:** Comparing Error Vector Magnitudes (EVMs) in Case 1 and Case 2 shows how NR interference affects HE receptions. EVMs approach -20 dB in Case 1 without NR interference. In Case 2, NR interference distorts constellations and lowers EVMs to -17 dB, suggesting poor reception. ACRs demonstrate NR-free channel separation by measuring power differences. The future investigation involves analyzing ACRs with HE waveforms as interferers and examining system behavior under different interference situations.
**Conclusion:** To reduce non-idealities in mobile communication transceivers, this thesis presents digital projection interpolation and Wiener-SAF for leakage route and receiver nonlinearity estimation.

**Keywords:** Mobile broadband traffic, heterogeneous networks, interference reduction methods, Simulink modeling, 5G communication interference.

## Introduction

The exponential growth in mobile broadband traffic in recent years can be attributed to the advancements in terminal capabilities. It is becoming increasingly difficult for mobile service providers to match the demand for apps requiring extremely high data rates [1]. Since spectrum is a limited resource, a variety of strategies are needed to boost network capacity and satisfy the ever-increasing demands for data rate [2]. The level of signal processing among the two devices will increase with additional antennas added to boost capacity. In order to boost capacity, operators also reduce the size of macro cells in urban and crowded locations by placing additional base stations, also known as eNodeBs (eNBs) [3]. The system will get more interfered with as a result. The issue with this approach is the fact that it is highly costly to add additional eNBs because of the high cost of real estate for tower placement and the requirement for costly driving testing to identify appropriate deployment locations. Adding Pico eNBs with distinct designs and minimal power are above the macro network is an alternate strategy. Heterogeneous networks (HetNet) are what we term them [4]. Depending on the requirements for local capacity, more pico nodes are added. But because the macro & pico broadcast at different powers, the interference caused by the addition to the pico node is more severe [5].

Because of the tiny transmit power and the intense interference that the macro eNB causes to user equipment (UE), the pico eNB's coverage is rather restricted [6]. The pico cell is quite close to if the downlink (DL) SINR noticed via the macro eNB and the pico eNB were the same; there is an equal signal with both noise and interference (SINR) border in this scenario. As a result, only a tiny portion the pico eNB is linked to UEs. The pico eNBs are not completely using the spectrum since there are not enough UEs [7]. Consequently, in order to transfer traffic from macro cells to pico cells and boost the network efficiency for HetNets, new methods must be developed. If more UEs are allowed to join the pico eNB, the network performs much better since further cell-splitting benefits are made possible by further leveraging the frequency resources. By adding a positive skew into the SINR found in relation with the pico eNB, increasing the number of UEs connected to the pico eNB [8]. The region and these UEs are known at the cell ranging extension & expansion (CRE) UEs they are associated with is referred to as the CRE region. For the UEs at the boundary between the macro and pico cells where the pico eNB serves, biassing, however, exacerbates the interference. Therefore, in order to truly profit from introducing the low power picos, effective interference mitigation measures are needed [9]. Multiple strategies are needed to reduce the impact significant disruption to a cellular network since one strategy is unable to completely mitigate the interference. In order to enhance the system's productivity, One such mitigation strategy is suggested, which is based on resource allocation and reception processing using an adjusted scheduling mechanism [10]. It measures average packet delay and packet delivery ratio in this work. In order to allocate resources, the performance is compared and examined using the interference suppression receiver, the round-robin (RR), proportionate fair (PF), & modified greatest weighting delay first (MLWDF) algorithms. Simulation results show what the MLWDF algorithm accomplishes. The highest delivery ratio and maximum throughput with the lowest average packet delay when compared to both PF & RR schedulers [11].

The literature provides a number of techniques for reducing signal interference during radio frequency (RF) interactions. To reduce interference at the receiver front-end, some techniques can include active interference cancellation in addition to filtering. Interference cancellation techniques fall into several categories among available methods, including domains of space, time, frequency, time-frequency, and coding [12]. Adaptive beamforming antenna arrays are used in space domain techniques to reduce interference caused by shifting the beam's direction as well as positioning nulls along the path of the interference. Fractional filters with indefinite impulse response (IIR) and impulse response (FIR) are used in timedomain approaches for adaptive filtering. These interference cancellation techniques do, however, need more complicated hardware and are only effective against narrowband interferers. Additionally, techniques in the frequency domain have been put forth to reject interference [13].

The latter has the significant disadvantage of needing Hardware that performs fast Fourier transforms (FFT), reverse FFTs, or wavelet transforms increases hardware complexity. Furthermore, windowing blocks are required to prevent excessive spectrum leakage, which suggests increased expenses [14]. Furthermore, estimating the instantaneous frequency of the interferer is necessary for time-frequency excision approaches, which suggests even more sophisticated hardware. It could also be necessary for estimating the interferer signal using a complex orthogonal-like Gabor expansion before removing it from the input [15].

## Experimental

## Method

The research design examines transmitter and receiver RF loss implications. The model evaluates I/Q imbalances, phase noise, and power amplifier non-linearity using Simulink with RF Block Set and WLAN Toolbox. Error vector magnitudes, spectrum masks, bandwidths, channel power, complementary cumulative distribution functions, and peaks-to-average power ratio are performance measures. Waveform creation, filtering, RF subsystem modeling, up-conversion, spectrum analysis, PAPR/CCDF computation, down-sampling, and demodulation are done packet-by-packet in Simulink. DSP, WLAN Toolbox, and RF Block Sets provide efficient accelerator and normal simulation. The research design uses Simulink modeling to evaluate superheterodyne transmitter architecture RF transmission impacts. Adjusted timing parameters match packet transmission (304.4 microseconds). RF transmission components like IQ modulators and power amplifiers are defined. Considerations include I/Q imbalance, phase noise, and power amplifier nonlinearity. The receiver model calculates EVM and demodulates signals, assessing subcarrier and overall EVM, while the RF transmitter model adapts baseband waveforms to RF configurations. Amplitude-to-amplitude modulations are assessed as nonlinear amplifier effects. Simulation results, including EVM graphs and spectrum masks, meet IEEE 802.11ax WLAN requirements.

*International Journal on Recent and Innovation Trends in Computing and Communication*
***ISSN: 2321-8169 Volume: 11 Issue: 9s***
***Article Received:** 30 April 2023 **Revised:** 20 June 2023 **Accepted:** 20 July 2023*

Simulink models are used to assess how RF impairments affect 802.11ax and 5G waveform receptions. I/Q imbalances and phase noise are assessed in the model's RF transmitter and receiver subsystems. The model simulates and evaluates constellation distortion by altering I/Q gains and phases mismatches. Error vectors, adjacent channel rejection, and packet error rates are measured to determine how adjacent 5G or 802.11ax signals affect RF reception. Simulations provide variable RF design and waveform testing by considering impairments. The Multi-band Combiners block adjusts frequencies for neighboring channels to measure neighboring Channel Ratios from oversampled waveforms. Simulink Stop Times capture EVM and constellation diagrams. The super-heterodyne RF Receivers Subsystem down-converts mixed signals. In addition to impairment effects, the model measures ACRs and RF interference from UHF transmitters and GNSS receivers. The importance for correct measured data is stressed in RFI analysis utilizing spec sheets. The study examines RF impairments and interference avoidance methods in detail.

**The Model Structure**

Figure 1 shows that the transmitter and receiver's response to radio frequency (RF) signal loss is the first step in our concept. The main component is the transmit model, which generates baseband waveforms using RF block sets and the WLAN Toolbox. This model successfully evaluates RF-related impairments such as I/Q imbalances, phase noise, and power amplifier non-linearity via performance measurements. Error vector magnitudes, spectral masks to prevent substantial interference in adjacent channels, occupy bandwidths representing integrated powers centred on assigned channel frequencies, channel power centred on assigned frequencies, complementary cumulative distribution functions indicating signal power probabilities above average levels, and Waveform generation, filtering, oversampling, RF transmitter subsystems for up-conversion, spectrum analysis for bandwidth and power assessments, PAPR and CCDF computations, and baseband waveform demodulation using DSP and WLAN Toolbox features and RF block sets supporting accelerators and normal simulation modes are done packet-by-packet in a SIMULINK model. The first process involves the creation of baseband waveforms. Up-conversion of these waveforms to carrier frequencies is simulated in the RF transmission portion. In the reception phase, RF measurements are taken and EVMs are calculated from the baseband waveforms by demodulation.

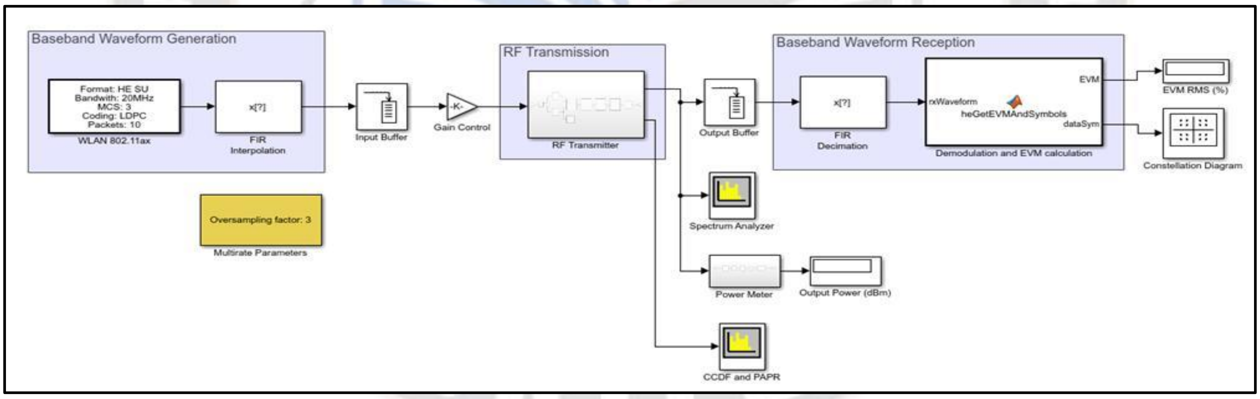


**Figure 1: Transmitter section**

**Generation of Baseband Signals**

Figure 2 shows WLAN blocks provide high-efficiency, standards-compliant single-user waveforms via user data parameters. Depending on the values of certain variables, these models save various user data structures in a dedicated workspace via callbacks. FIR interpolation prevents oversampling and filters waveforms, illustrating the effect of high-power amplifiers on spectrum emissions beyond the audible range. At the block outputs of the RF transmitter subsystem, FIR decimation blocks downsample the waveform to the original sample rate. Parameters for a series of FIR decimation and interpolation blocks may be specified using a straightforward interface thanks to multi-rate parameter blocks. The user-defined settings in the waveform parameters, saved by callbacks, assure adherence to WLAN standards while the FIR interpolation and decimation blocks play crucial roles in analyzing and changing the spectral properties of the sent signals.

*International Journal on Recent and Innovation Trends in Computing and Communication*
***ISSN: 2321-8169 Volume: 11 Issue: 9s***
***Article Received:** 30 April 2023 **Revised:** 20 June 2023 **Accepted:** 20 July 2023*

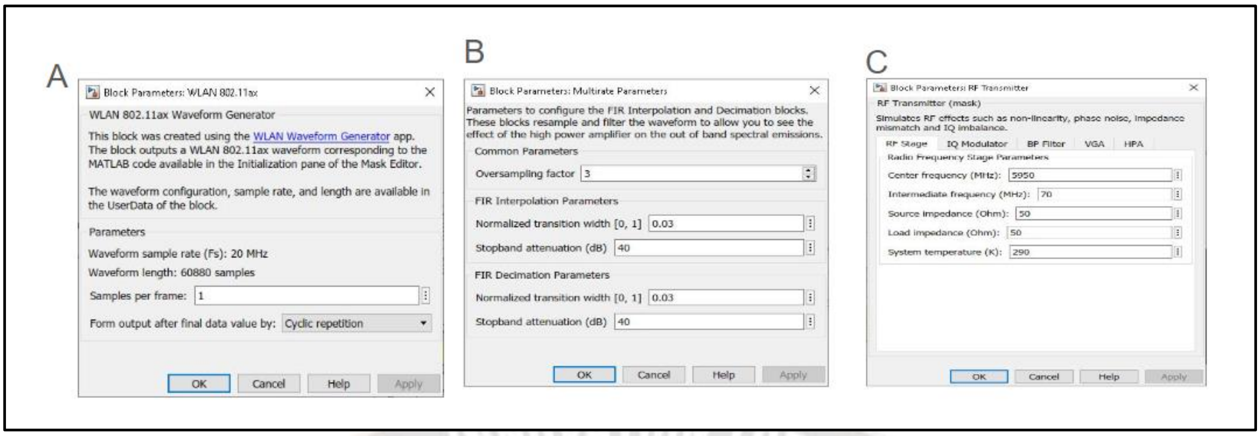


**Figure 2: Block parameters configuration**

**Transmission of RF**

The RF transmission block subsystem functions based on the design of a superheterodyne transmitter as presented in Figure 3. The up-conversion process converts waveforms into carrier frequencies, and this model includes numerous crucial RF components to quantify the impacts of this transformation. Mixers, phase shifters, and local oscillators are just a few of the parts that make up the IQ modulator, which modulates both the I and Q components. The frequency content of the signals is refined by integrated bandpass filters, and their power is amplified by integrated power amplifiers. Notably, the input back-off levels of the High Power Amplifier (HPA) may be adjusted via variable gain amplifiers included in the RF transmitters' subsystem blocks. The up-conversion process inside the superheterodyne transmitter may be accurately modeled with this complete design, allowing for a full investigation of the RF components and their roles and interactions in the transmission chain.

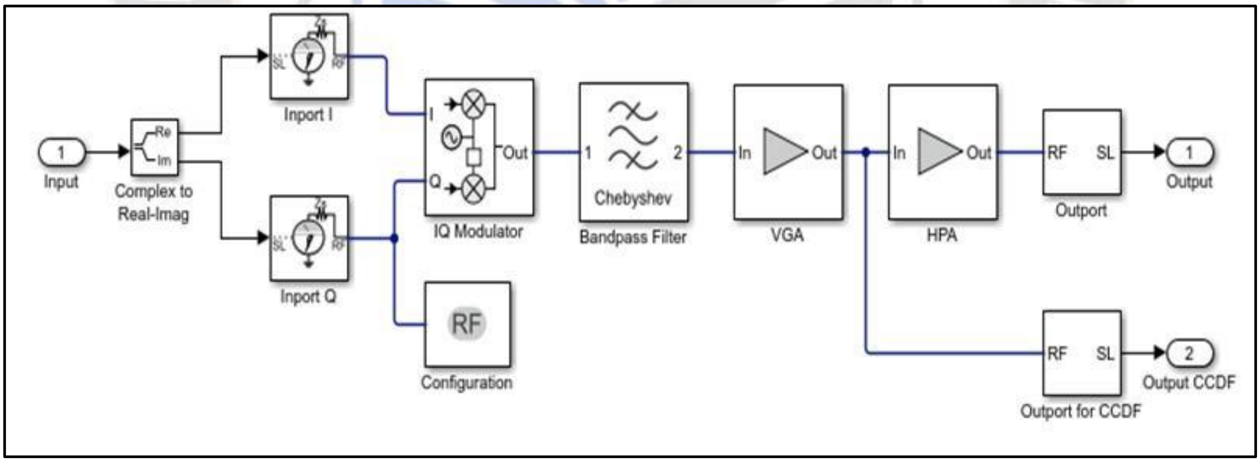


**Figure 3: Super heterodyne RF transmitter structure**

**Effecting of Non-linear Amplifier**

The effect of nonlinearity in a High Power Amplifier (HPA) on the evaluation of EVM may be characterized by measuring amplitude-to-amplitude modulations as shown in Figure 4. Nonlinear effects of the HPA may be better understood by this evaluation, which assesses the response of the output power to variations in the input power. To evaluate the effect of nonlinearity on the overall performance of the system, especially in terms of Error Vector Magnitude (EVM) measurements, amplitude-to-amplitude modulations provide a crucial metric by quantifying the link between output power levels and input power levels.

*International Journal on Recent and Innovation Trends in Computing and Communication*
***ISSN: 2321-8169 Volume: 11 Issue: 9s***
***Article Received:** 30 April 2023 **Revised:** 20 June 2023 **Accepted:** 20 July 2023*

---

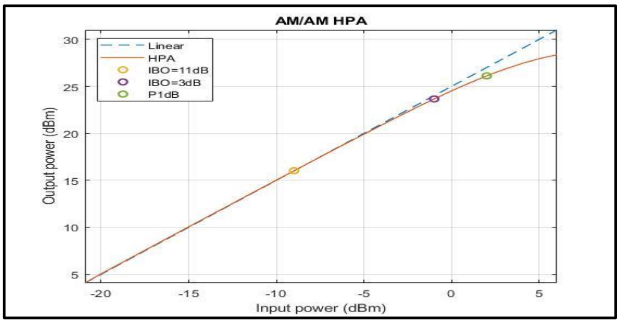


**Figure 4: HPA amplitude to amplitude modulations evaluation**

### Effecting of Non-linear Amplifier

Figure 5 shows High Power Amplifiers (HPAs), chosen Input Back-Off (IBO) values are based on P1dB. EVM findings at different HPA operating points are used to evaluate HPA effects on RF transmitter subsystem blocks. For example, comparing IBO = 11 dB, showing linear HPA operation, to IBO = 3 dB, indicating saturation, shows the amplifier's effects. Default settings keep VGA gains below 15 dB to manage IBO levels linearly. Set VGA block power boost to 5 dB for IBO = 11 dB. EVM computation, constellation diagram drawing, and HPA system performance assessment are done on one packet from simulations.

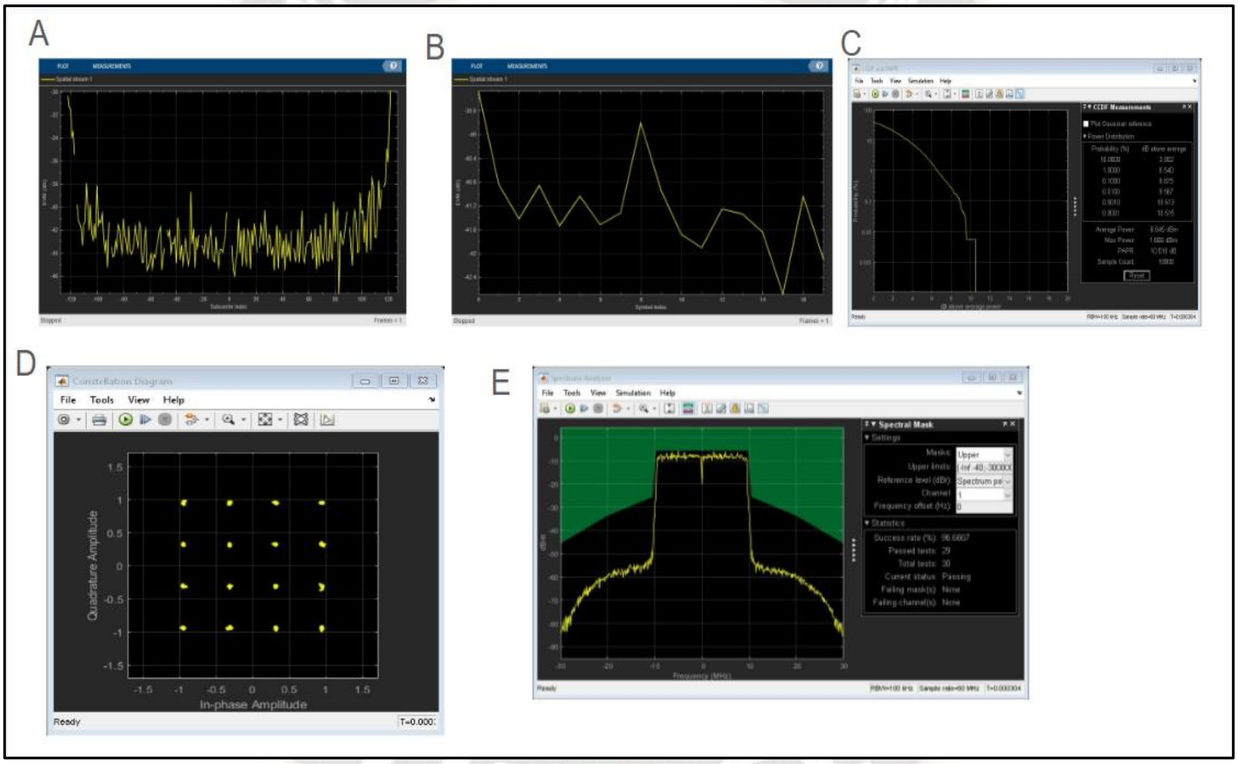


**Figure 5: PLOT measurement of EVM waveforms VS subcarrier indexing**

### Probability of power distribution

Figure 6 shows constellation diagrams, which include the GSM spectrum mask, which describes the received waveforms in terms of probability distributions. By IEEE P802.11ax/D7, we provide EVM charts vs subcarrier and symbol indexing. High-efficiency single-user (HE SU) Physical Protocol Data Units (PPDUs) using double carrier modulations (DCMs) characteristics, corresponding to 16-QAM (1/2), are allowed to have a comparable EVM of -16 dB in conformity with these specifications. The total EVM of -41 dB is far lower than what is needed. Setting the VGA block power gains to 13 dB for the stated IBO level ensures compliance with IEEE P802.11ax/D7.0 standards, notwithstanding the non-linearity of the High Power Amplifier (HPA) at IBO = 3 dB.

*International Journal on Recent and Innovation Trends in Computing and Communication*
***ISSN: 2321-8169 Volume: 11 Issue: 9s***
***Article Received:** 30 April 2023 **Revised:** 20 June 2023 **Accepted:** 20 July 2023*

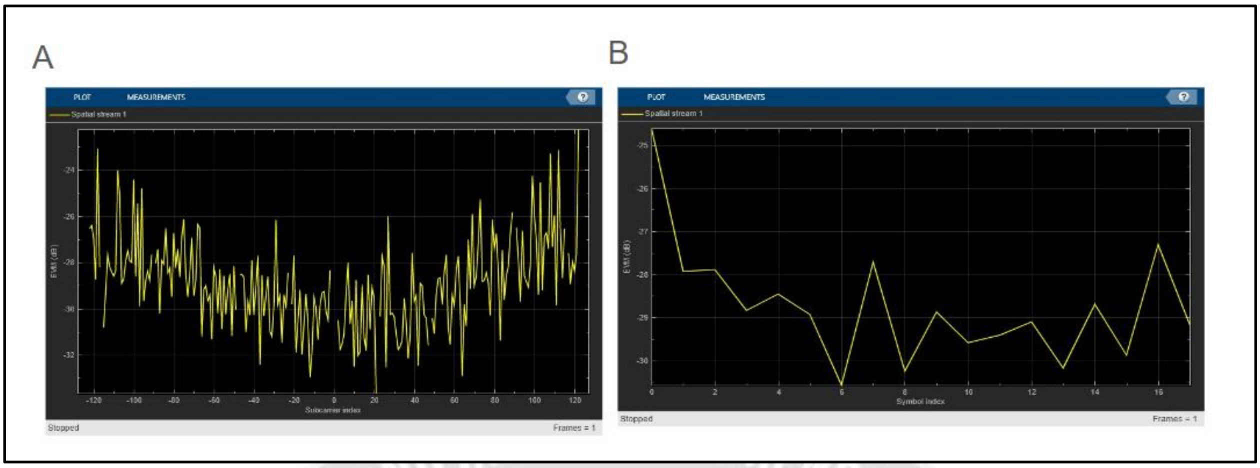


**Figure 6: Probability of power distribution**

**GSM mask of received signals**

Probability distribution, Q constellation diagrams, /GSM masks, and I illustrate receiver performance in Figure 7. These representations provide a complete picture of signal behavior and quality. The probability distribution shows signal fluctuations by displaying data statistics. In-phase and quadrature constellation diagrams show the signal's amplitude and phase, revealing its modulation scheme and impairments. The GSM mask also visually checks incoming signals for spectrum conformity, assuring compliance and reducing interference. These performance indicators show the receiver's capacity to catch and analyze broadcast signals under different settings.

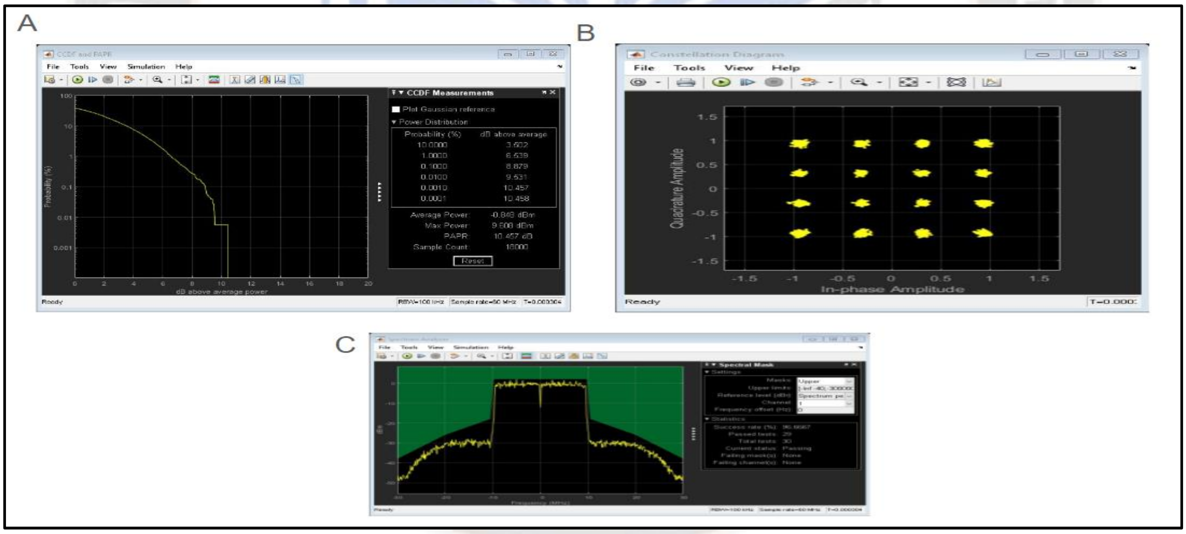


**Figure 7: GSM mask of received signals**

**Receiver SIMULINK Modelling Structures**

Signal processing components are in the GSM receiver model as represented in Figure 8. Baseband Waveform Generation creates and integrates 802.11ax and 5G baseband waveforms. After then, RF Reception mimics down-conversion effects to convert the combined waveforms to intermediate frequencies. Preparing the signal for processing requires this step. After that, the Baseband Waveforms Reception portion calculates crucial metrics like EVMs and PERs. These measures determine signal fidelity and dependability, revealing the GSM system's receiver's performance and accuracy under various operating settings. These coupled components provide a complete receiver model, guaranteeing the system can handle and comprehend mixed waveforms.

*International Journal on Recent and Innovation Trends in Computing and Communication*
***ISSN: 2321-8169 Volume: 11 Issue: 9s***
***Article Received:** 30 April 2023 **Revised:** 20 June 2023 **Accepted:** 20 July 2023*

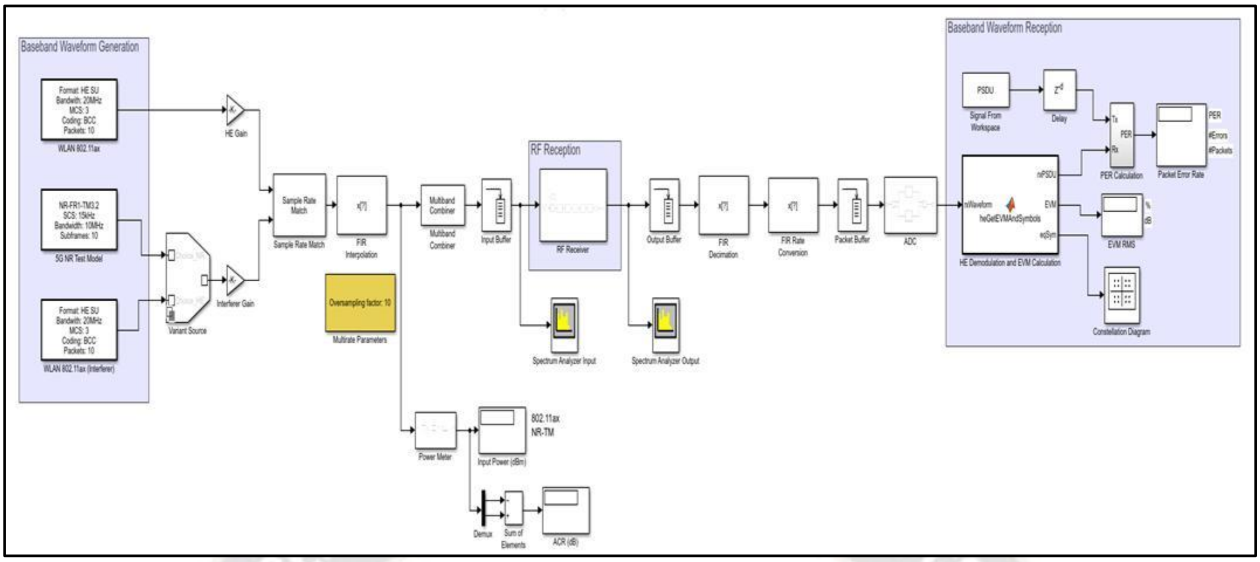

**Figure 8: Receiver SIMULINK Modelling Structures**

**Receptions of Radio Frequency**

The Radio Frequency Receivers Subsystem blocks use superheterodyne receiver design. This model characterizes essential RF components by down-converting signals to intermediate frequencies which are shown in Figure 9. These components refine and isolate the required frequency range via IF and RF bandpass filters. The LNA boosts signal strength while reducing noise. Baseband signal extraction is done via mixers, phase shifters, and local oscillators in the demodulation step. The combined signals are down-converted effectively by this design, ready them for receiver subsystem processing. The model explains how the superheterodyne design affects down-conversion and signal extraction in the RF receiver system by describing each RF component.

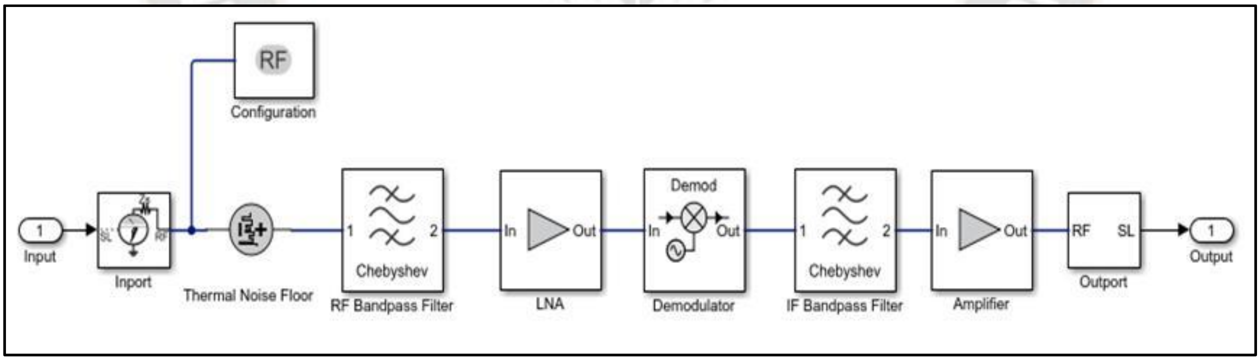


**Figure 9: RF superheterodyne receiver**

**RF Requirement vs. Compatibilities**

Separated RF units must meet performance specifications for in-band and out-of-band operations. Individual unit testing may misdiagnose Radio Frequency Interference (RFI) concerns that may not exist when numerous RF systems are linked. MIL-STD-461's failure to cover all RF system use scenarios shows that profitability and military criteria do not ensure compatibility. RF kits, antennas, filters, and amplifiers may not be compatible even if they meet MIL-STD-461 at the unit level. Simulations and tests must be properly planned to discover and resolve problems to avoid unfamiliarity and RFIs. Emerging Electromagnetic Interference Technologies (EMITs) specialize on RFI issues and use a multi-fidelity

*International Journal on Recent and Innovation Trends in Computing and Communication*
***ISSN: 2321-8169 Volume: 11 Issue: 9s***
***Article Received:** 30 April 2023 **Revised:** 20 June 2023 **Accepted:** 20 July 2023*

method that blends higher-fidelity data with parametric models–an crucial skill given the lack of high-fidelity data for all components during initial study. Block diagrams highlight filters, wires, amplifiers, and multiplexers that cause UHF transmitter-GNSS receiver interference shown in Figure 10. Some component makers provide S-parameter measurements online, like Mini-Circuit's bandpass filter model. Diverse solver methods in HFSS products allow modeling of broad-band antenna-to-antenna couplings, essential for interference analysis.

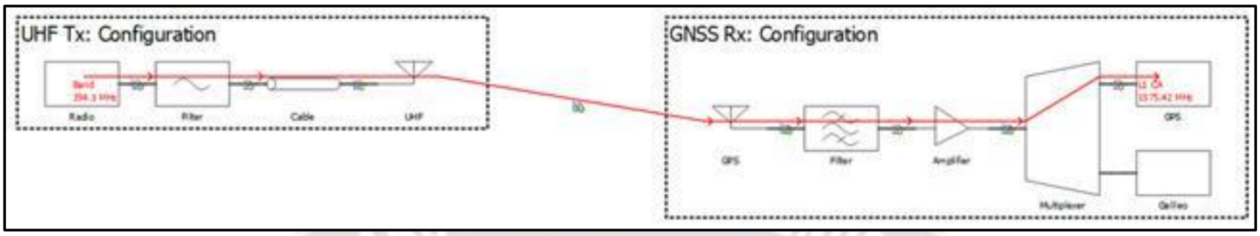


**Figure 10: Interference problems between a UHF transmitter and a GNSS receivers**

**Limitation Data could limit the RFI Analyzing**

Using data from specification sheets or DD 1494 to create models of a transmitter and receiver provides two main difficulties. First, since these sources provide restricted and conventional information, RFI models generally make many incorrect interference predictions. Second, models made from spec sheets and DD 1494s lack key characteristics, omitting interference issues. Comparing EMA ARMS data to spec sheet data for a UHF transmitter model shows a substantial difference in indicated Figure 11. Spec sheets properly measure the 2nd and 3rd harmonics; however following harmonics are up to 50 dB higher. Spec sheets for harmonic amplitudes may foresee interference issues that don't occur. Spec sheets also omit transmitter false emissions restrictions, which are crucial for controlling many large false emissions.

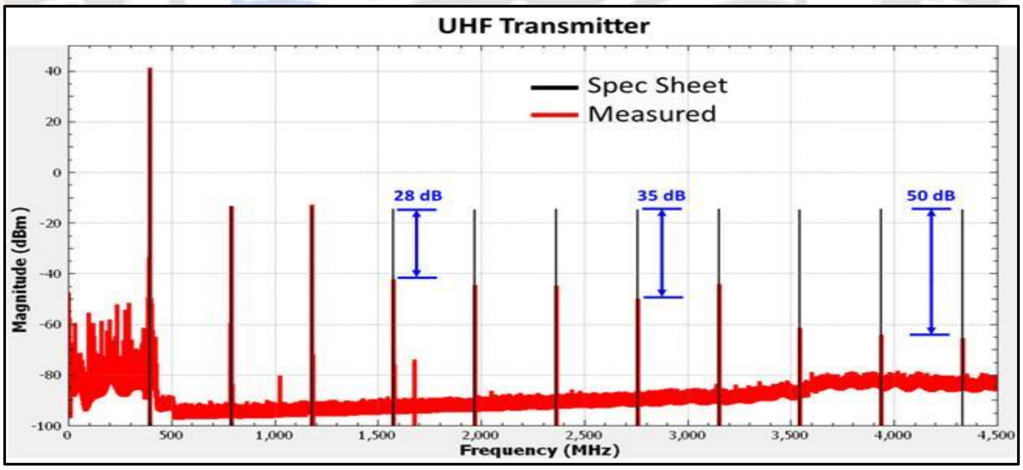


**Figure 11: Comparison among models of UHF transmitters of spec sheets data and measures information collect via EMA ARMS.**

**GNSS receivers tuned to L1**

Figure 12 presents that Spec sheets and measured data for a GNSS receiver set to L1 show significant discrepancies when assessing receiver performance. The measured data shows far more discrimination than the selectivity provided in the spec sheets, as seen in the figure. However, the spec sheet model is 60 dB off. An out-of-band response at 1280 MHz is another aspect not fully reflected in the spec sheets. This emphasizes the need of using measured data to better understand receiver

*International Journal on Recent and Innovation Trends in Computing and Communication*
***ISSN: 2321-8169 Volume: 11 Issue: 9s***
***Article Received:** 30 April 2023 **Revised:** 20 June 2023 **Accepted:** 20 July 2023*

behaviors and ensure that simulations and models match real-world performance.

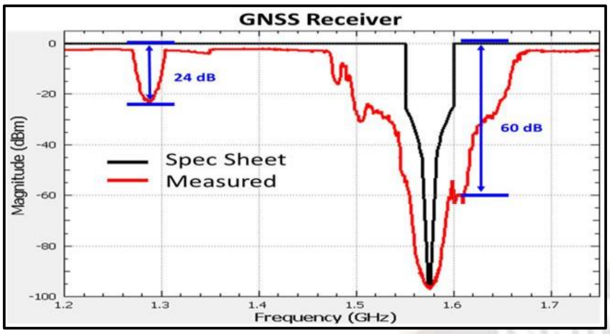


**Figure 12: Comparison between the spec sheets information and measures information for a GNSS receivers tuned to L1**

**EMIT simulations at 4th harmonics of the UHF transmitters**

To demonstrate the effectiveness of measurement information in Radio Frequency Interference (RFI) modeling, assume a UHF transmitter at 390 MHz and a GNSS receiver at L1 (1575.42 MHz) without interference. The UHF transmitter's 4th harmonics are at 1560 MHz, near L1 shown in Figure 13. However, the GNSS receiver's specs state that its selectivity prevents interference. EMIT simulations show that the UHF transmitter's 4th harmonics are 10 dB below the receiver's vulnerability at 1560 MHz. In contrast, EMIT models predict 35.6 dB interference concerns using measurement data. The spec sheets model is 46 dB off, highlighting the need of correct measurement information in RFI simulation dependability.

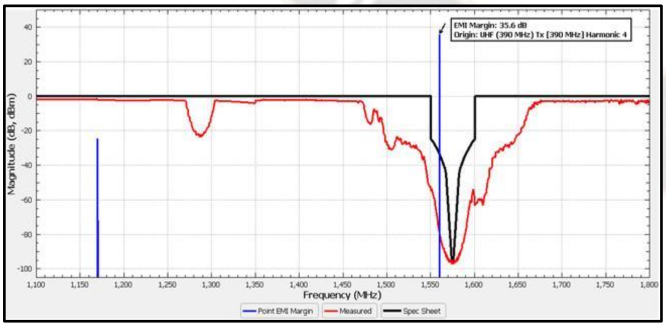


**Figure 13: EMIT simulations at 4th harmonics of the UHF transmitters**

**QAM modulations under multi orders AWGN channels**

Electro Magnetic Application (EMA) tests airplanes, ground vehicles, ships, satellites, and rockets for Radio Frequency Interference (RFI) in Figure 14. EMA's Advanced RFI Measurement System (ARMS) technology gathers detailed transmitter and receiver data, revealing many interference concerns that could otherwise go undetected until final testing or deployment. Signal transmission and demodulation methods are examined in Additive White Gaussian Noise (AWGN) channels with different orders. Quadrature Amplitude Modulation (QAM) with many orders under AWGN channel noise shows that 64 QAM is best for the suggested modeling. RFI exams across communication systems are more accurate and effective when modulation methods and noise characteristics are well understood.

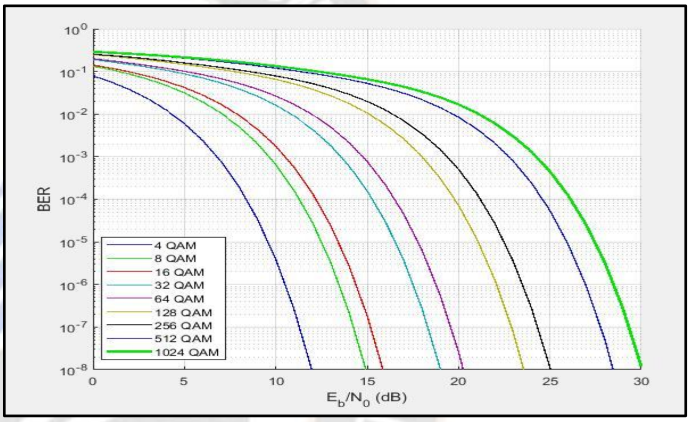


**Figure 14: QAM modulations under multi orders AWGN channels**

**Results**

Error Vector Magnitudes (EVMs) are compared between two scenarios, one without NR interference (Case 1) and one with NR interference (Case 2), to define the effects of NR interferences on HE receptions.

In Case 1, if there is no NR interference, the Interferers Gains blocks' parameters are set to zero. Simulations are run to capture one packet, and the received waveform performance without interference is displayed in Figure 15. Without any outside interference, the EVMs reach about -20 dB. In Case 2, NR interferences are enabled by assigning non-zero values to the Gains parameters in the Interferers Gains blocks.

*International Journal on Recent and Innovation Trends in Computing and Communication*
***ISSN: 2321-8169 Volume: 11 Issue: 9s***
***Article Received:*** *30 April 2023* ***Revised:*** *20 June 2023* ***Accepted:*** *20 July 2023*

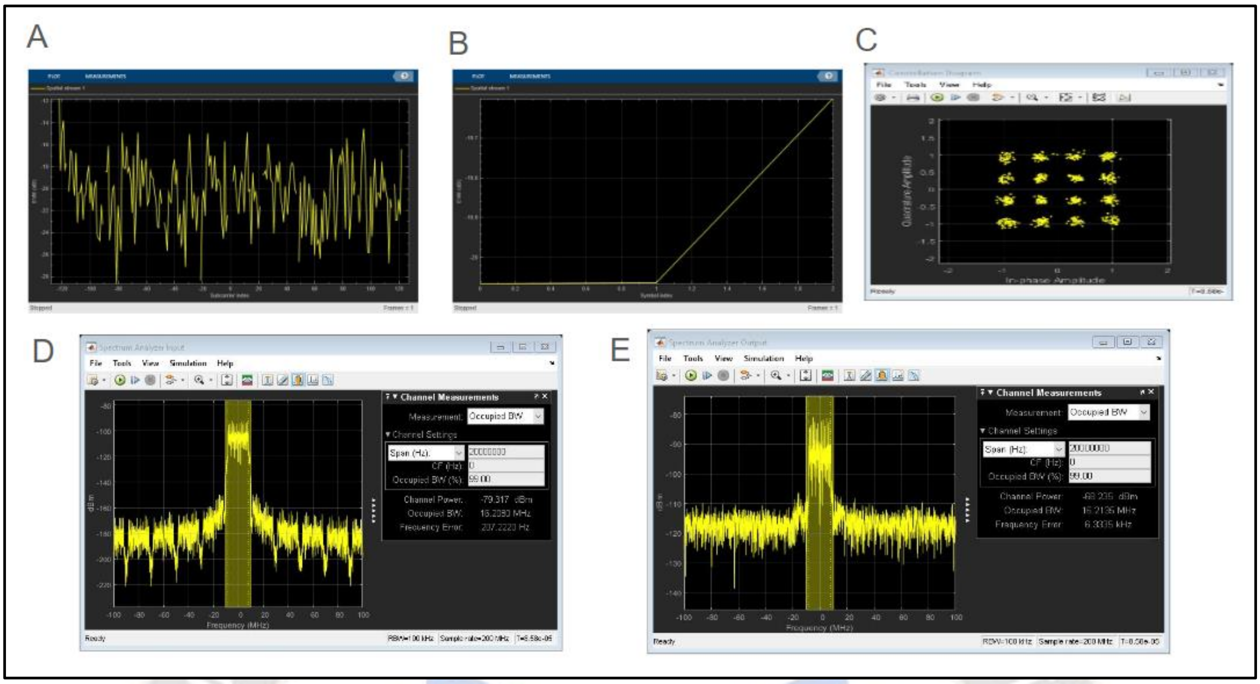


**Figure 15: EMV without interference case 1**

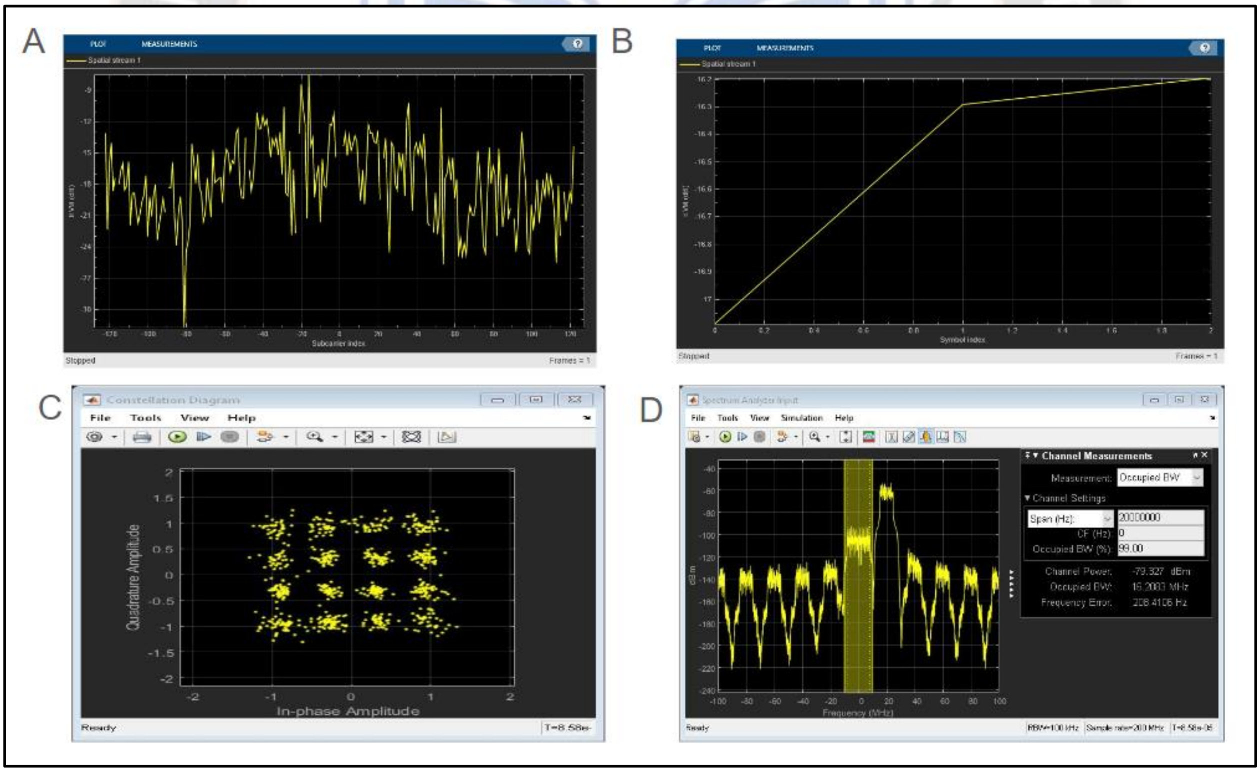


**Figure 16: Frequency mask without interference case 1**

For PSDUs of length 4096 octets, the ACRs are calculated when the Packet Error Rates (PERs) are close to 10%. The constellations diagrams are more distorted and all EVMs are roughly -17 dB, compared to the case without interference in Figure 16. In the presence of NR noise, the ACRs are around 38 dB. Gains values of the Interferers blocks are adjusted to around -72.4 dB in order to measure the ACRs when the interferers are HE waves. The influence of NR interferences

*International Journal on Recent and Innovation Trends in Computing and Communication*
*ISSN: 2321-8169 Volume: 11 Issue: 9s*
***Article Received:** 30 April 2023 **Revised:** 20 June 2023 **Accepted:** 20 July 2023*

on HE waveform reception is revealed through these simulations. In Case 1, where NR interference is absent, the received waveform has unblemished features, with EVMs hovering around -20 dB. Constellation diagrams become more distorted in Case 2 due to NR interference and EVMs drop to around -17 dB. This indicates that there is NR interference present, which is degrading the reception quality. The ACRs, which measure the powers disparities between the intended signals and interfering signals on adjacent channels, are vital in evaluating the system's performance. Good channel isolation is shown by the ACR value of roughly 38 dB in the absence of NR interference. Future analysis comprises analyzing ACRs when the interferers are HE waveforms, altering gains levels, and studying the system's behavior under diverse interference conditions. These simulations give a full picture of the system's stability and serve as a foundation for fine-tuning and optimization in real-world scenarios with a wide range of interference.

**Discussion**

We provide a new ultra-wideband low-cost transmit/receive design that supports many users and has lower power and hardware needs [16]. It also has interference mitigation features. In particular, a unique encoding technique is presented to distribute signals across wide bandwidths, provide secure transmission, and reduce interference. The suggested high-speed data system design is described in full in the study [17]. Additionally, simulations with eight users at once high-power interferers are present and incorporated. An examination of the noise was done for both receiver and transmitter chains in order to evaluate the effectiveness and influence of the encoding/decoding process. In particular, bit-error curves appear at various systemic phases. The improvement in interference margin ratios was at least 16 dB, according to the tests [18].

The last ten years have seen the development of silicon-based phase array technology, which is beginning to influence military and commercial wireless applications. Over the course of the next ten years, large-scale technique for multiple-input multiple-output (MIMO) will mature and gain traction, mostly due to the growth of wifi networks of the next generation [19]. Multi-input multiple-output arrays are susceptible to interference between the radio-frequency (RF) and analogue ends because they make use of digital array signal processing. Traditional digital MIMO reception arrays lack analog/RF interference mitigation, which leads to designs with analogue & Front ends for RF receivers and converters from analogue to digital that are highly dynamic and power-hungry [20]. The paper presents recently developed methods for digital MIMO receivers' decrease of spatio-spectral interference in the RF and analogue domains. The techniques proposed are characterised by their flexibility, tunable across operating frequency, scalability, low cost, size, and electrical overheads, and experimental validation using a 65-millimeters complementary metal-oxide-semiconductor (CMOS) four-element receiver front-end set integrated circuit (IC) prototype operating between 0.1 and 1.7 GHz [21].

In a wireless cell network, a heterogeneous network is made up of pico cells superimposed over the macro cell service region [22]. By further recycling the spectrum, the pico cells can be utilised to improve the capacity of a homogenous network. However, because the transmitting capacity of a pico cell is limited, more users will often be paired with the macro cell. Using range extension strategies like as biassed association, the number of those associated with the pico cell is increased [23]. This will result in significant interference for the pico cell's cell edge users from the macro cell, which will lower throughput outcomes in the area where the cell range extends. This study proposes several scheduling strategies combined with receiver processing for interference reduction in order to increase the system's throughput performance. For resource allocation, a performance comparison and analysis are conducted between proportional fair, modified greatest weighted delay first (MLWDF), and round robin algorithms. It is demonstrated that the MLWDF methodology produces the most packets in an optimal delivery ratio at the maximum throughput and lowest average latency [24].

**Conclusion**

Constraints in area, power, and cost make mobile communications transceivers non-ideal. In situations like concurrent WiFi transmissions during FDD operations, even-order Inter-Modulation Distortions (IMDs) might damage direct conversion receivers. These IMDs can significantly lower receiver SNR, raising Bit Error Rates. This thesis addresses this issue in two ways. First, a fully digital projection interpolation and complex-value Wiener-SAF method to estimate transmit-receive leakage routes and receiver non-linearities. Second, mixing-signals architectures capture interferers through an Auxiliary receiver for digital reproduction and cancelation of receiver intermodulation products. Future research could refine SAF learning algorithms, expand to high-order intermodulation product cancellation, and produce fully digital odd-order intermodulation solutions. Research on holistic learning schemes like Kernel Adaptive Filters (KAFs), neural networks (NNs), or tensor-based estimation algorithms could improve the algorithm's frequency-dependent I/Q imbalance compensation and statistical properties of LTE/NR signals for optimization. Understanding the algorithm's complexities could improve implementations and frequency-dependent I/Q imbalance compensation, motivating further research.

## References

1. Feng, M.J., Jiang, T., Chen, D. and Mao, S.W. (2014) Cooperative Small Cell Networks: High Capacity for Hotspots with Interference Mitigation. IEEE Wireless Communications, 21, 108-116.
2. Damnjanovic, A., et al. (2011) A Survey on 3GPP Heterogeneous Networks. IEEE Wireless Communications, 18, 10-21.
3. Ghosh, A., Ratasuk, R., Mondal, B., Mangalvedhe, N. and Thomas, T. (2010) LTE-Advanced: Next Generation Wire-less Broadband Technology. IEEE Wireless Communications, 17, 10-22.
4. Pauli, V., Naranjo, J.D. and Seidel, E. (2010) Heterogeneous LTE Networks and Inter-Cell Interference Coordination. Nomor Research GmbH, Munich, 1-9.
5. Gerhard, W., et al. (2015) 5G Now Final MAC/Networking Concepts. 5GNow_D4.2_Final.
6. Supratim, D., Pantelis, M., Jerzy, M. and James, P.S. (2014) Algorithms for Enhanced Inter-Cell Interference Coordi-nation (eICIC) in LTE HetNets. IEEE/ACM Transactions on Networking, 22, 137-150.
7. Andrews, J.G., Choi, W. and Heath Jr., R.W. (2007) Overcoming Interference in Spatial Multiplexing MIMO Cellular Networks. IEEE Wireless Communications, 14, 95-104.
8. Balint, C., Budura, G. and Marza, E. (2010) Scheduling Techniques Evaluation in LTE systems with Mixed Data Traffic. Proceedings of the 9th International Symposium on Electronics and Telecommunications, Timisoara, 11-12 November 2010, 221-224.
9. Gomez, K., Goratti, L., Granelli, F. and Rasheed, T. (2014) A Comparative Study of Scheduling Disciplines in 5G Systems for Emerging Communications. Proceedings of the 1st International Conference on 5G for Ubiquitous Connectivity, Akaslompolo, December 2014, 1-6.
10. T. D. Werth, C. Schmits, R. Wunderlich, and S. Heinen, ‘‘An active feedback interference cancellation technique for blocker filtering in RF receiver front-ends,’’ IEEE J. Solid-State Circuits, vol. 45, no. 5, pp. 989–997, May 2010.
11. A. Raghavan, E. Gebara, E. M. Tentzeris, and J. Laskar, ‘‘Analysis and design of an interference canceller for collocated radios,’’ IEEE Trans. Microw. Theory Techn., vol. 53, no. 11, pp. 3498–3508, Nov. 2005.
12. G. Karawas, K. Goverdhanam, and J. Koh, ‘‘Wideband active interference cancellation techniques for military applications,’’ in Proc. 5th Eur. Conf. Antennas Propag. (EUCAP), Apr. 2011, pp. 390–392.
13. J. T. Chiang and Y.-C. Hu, ‘‘Dynamic jamming mitigation for wireless broadcast networks,’’ in Proc. 27th Conf. Comput. Commun., Apr. 2008, pp. 1211–1219.
14. H. Yamaguchi, ‘‘Active interference cancellation technique for MB-OFDM cognitive radio,’’ in Proc. 34th Eur. Microw. Conf., vol. 2, Oct. 2004, pp. 1105–1108.
15. Y.-R. Chien, ‘‘Design of GPS anti-jamming systems using adaptive notch filters,’’ IEEE Syst. J., vol. 9, no. 2, pp. 451–460, Jun. 2015.
16. M. Jones, ‘‘The civilian battlefield: Protecting GNSS receivers from interference and jamming,’’ Inside GNSS, vol. 6, no. 2, pp. 40–49, Mar./Apr. 2011.
17. Y. D. Zhang and M. G. Amin, ‘‘Anti-jamming GPS receiver with reduced phase distortions,’’ IEEE Signal Process. Lett., vol. 19, no. 10, pp. 635–638, Oct. 2012.
18. T. D. Werth, C. Schmits, R. Wunderlich and S. Heinen, "An active feedback interference cancellation technique for blocker filtering in RF receiver front-ends", IEEE J. Solid-State Circuits, vol. 45, pp. 989-997, May 2010.
19. A. Raghavan, E. Gebara, E. M. Tentzeris and J. Laskar, "Analysis and design of an interference canceller for collocated radios", IEEE Trans. Microw. Theory Techn., vol. 53, no. 11, pp. 3498-3508, Nov. 2005.
20. G. Karawas, K. Goverdhanam and J. Koh, "Wideband active interference cancellation techniques for military applications", Proc. 5th Eur. Conf. Antennas Propag. (EUCAP), pp. 390-392, Apr. 2011.
21. A. Hajimiri, H. Hashemi, A. Natarajan, X. Guan and A. Komijani, "Integrated phased array systems in silicon", Proc. IEEE, vol. 93, no. 9, pp. 1637-1655, Sep. 2005.
22. A. Natarajan, A. Komijani, X. Guan, A. Babakhani and A. Hajimiri, "A 77-GHz phased-array transceiver with on-chip antennas in silicon: Transmitter and local LO-path phase shifting", IEEE J. Solid-State Circuits, vol. 41, no. 12, pp. 2807-2819, Dec. 2006.
23. A. Babakhani, X. Guan, A. Komijani, A. Natarajan and A. Hajimiri, "A 77-GHz phased-array transceiver with on-chip antennas in silicon: Receiver and antennas", IEEE J. Solid-State Circuits, vol. 41, no. 12, pp. 2795-2806, Dec. 2006.
24. A. Natarajan, A. Komijani and A. Hajimiri, "A fully integrated 24-GHz phased-array transmitter in CMOS", IEEE J. Solid-State Circuits, vol. 40, no. 12, pp. 2502-2514, Dec. 2005.